Fatigue, Creep and Fracture

EFFECTS OF MICROSTRUCTURE ON LOW CYCLE FATIGUE PROPERTIES IN HIP TREATED Al-Si-Mg BASE CAST ALUMINUM ALLOYS

Shinji Kumai, Koji Katsumata and Akikazu Sato

Department of Materials Science and Engineering
Tokyo Institute of Technology
4259 Nagatsuta, Midori-ku, Yokohama 226-8502 Japan

ABSTRACT Low cycle fatigue tests were performed for two plastic strain amplitudes ($1x10^{-4}$ and $5x10^{-4}$) in sand cast and HIPed (hot isostatic pressing treated) JIS AC4CH (AA A356) aluminum alloy castings. Cyclic hardening took place in different manner to give various cyclic stress levels depending on the eutectic Si particle morphology, aging condition and applied plastic strain amplitude.

Keywords: *low cycle fatigue, A356 alloy, HIP, cyclic hardening*

1. INTRODUCTION

Aluminum alloy castings have become a viable alternative in structural applications for ground-vehicles. It is because that the flexibility of the casting can provide great advantage in reducing overall manufacturing costs in addition to the merit of weight reduction. Recently the use of the aluminum alloy castings in nontraditional applications has been facilitated, in which improved fatigue resistance is required [1]. Elimination of casting defects, such as internal voids by HIPing has a generally favorable effect on the smooth-bar fatigue life of Al-Si-Mg base alloys. In the HIPed alloy, fatigue crack has been reported to initiate from active slip planes and eutectic Si particles [2]. In such situation the conventional life prediction based on the morphology of pre-existing casting defects is no longer applicable. This means that we need to pay much more attention to the effects of microstructure on fatigue properties with improvements in casting quality. In the present study effects of microstructure on low cycle fatigue properties are examined using the sand cast and HIPed Al-Si-Mg base alloys. The low cycle fatigue test, the classical short-life strain-based fatigue test, is not only the basic method in investigating fatigue mechanism, but is also widely used to fatigue design in ground-vehicle industries [3].

2. EXPERIMENTAL PROCEDURES

2.1 Materials

Materials used in the present study are JIS AC4CH (AA A356) cast aluminum alloys, which are one of the members of the dual-phase Al-Si-Mg system. Chemical compositions of the alloy was 7%Si, 0.32%Mg, 0.16%Ti, 0.1%Fe and bal. Al (wt%). Castings were fabricated at the Advanced Materials Research Laboratory, Hitachi Metals, Ltd.. The materials were melted at

993K and cast into the sand mold located in the pressure vessel. The melt was cooled at a relatively slow cooling rate under a 1MPa pressure. The size of the resultant castings were 170x120x16 (mm). For some castings, 100ppm of strontium was added to the melt just before casting. This modification treatment caused morphological change in eutectic Si particles, as will be shown later. The resultant castings were HIPed with the applied pressure of 100MPa over a period of 1h at 773K in Ar atmosphere to reduce casting defects such as shrinkage and porosities. Figure 1(a) shows microsturucture of the casting modified with Sr but un-HIPed. Porosities are observed at the inter-dendritic region. While, for the HIPed materials, which were used in the present study, very few casting defects are observed both in the modified (Fig. 1 (b)) and the un-modified (Fig.1 (c)) castings. The average dendrite arm spacing (DAS) was comparable in all the castings, and was about 60μm. However, difference is evident in the eutectic Si particle morphology. The modified casting consisting of the primary Al dendrite contains globular eutectic Si particles, while the un-modified casting contains coarse irregular needle-like eutectic Si particles.

2.2 Test specimens and heat treatment

The HIPed castings were cut into rectangular bars with shoulders (gage section: 16x5x4mm) for low cycle fatigue tests. These specimens were also used for monotonic tensile tests. They were solution treated at 793K for 8h and water quenched. After holding at a room temperature for 24h, the specimens were aged at 463K. Two kinds of aging time, 1h and 20h were chosen in the present study referring to the age hardening curves obtained in advance. Each aging condition is called UA (under aged) and OA (over aged) hereinafter. According to the previous studies made on the same alloy, the UA is strengthened by the GP zone which are shearable by dislocations. On the other hand, the strengthening of the OA results from combined precipitation of the GP zones and semi-coherent intermediate precipitates β'. The latter are considered to be un-shearable by the dislocations.

Prior to fatigue testings monotonic tensile tests were performed at the constant strain rate of 8.3×10^{-5} s^{-1} in order to examine static tensile properties. Typical stress-strain curves are shown in Fig. 2 for 4 kinds of specimens treated here; modified UA, modified OA, un-modified UA and un-modified OA. The OA materials have slightly higher flow stress values. The un-modified materials exhibit significantly higher flow stress and strain hardening rate, but poor ductility compared to the modified materials.

2.3 Low cycle fatigue tests and microstructural observation

Surfaces of the specimens were mechanically polished with fine grain diamond-paste. Polishing was made parallel to the longitudinal axis to remove any scratches which become origins of stress concentration leading to early stage crack initiation in the fatigue tests. The tests were performed by controlling the plastic strain amplitude in a fully-reversed mode with the stress ratio R = -1, using a Saginomiya servo-hydraulic testing machine with a sinusoidal wave form at a room temperature in air. The tests were started at a low frequency (0.05 Hz) and continued at the

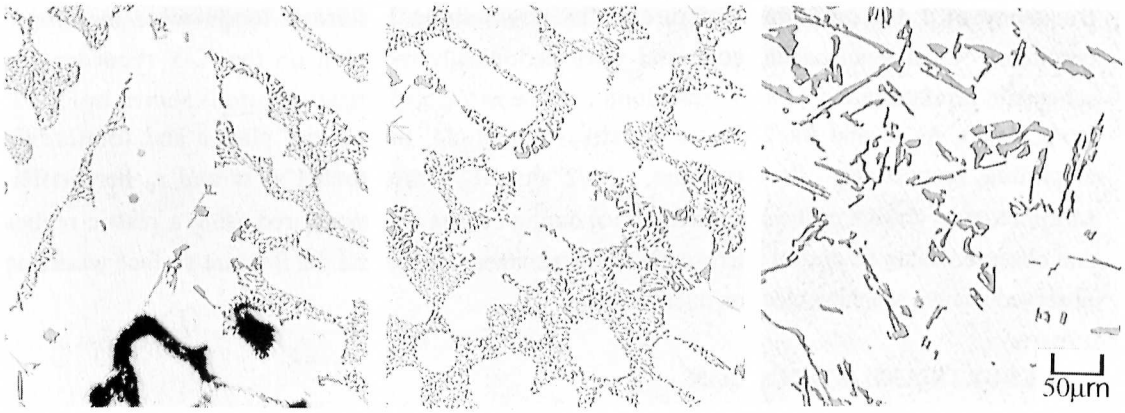

(a) modified & un-HIPed (b) modified & HIPed (c) un-modified & HIPed

Fig. 1 Microstructure of the sand cast AC4CH (A356) alloys.

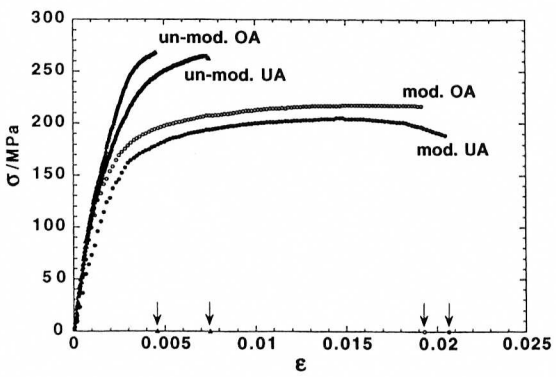

Fig. 2 Stress-strain curves obtained by monotonic tensile tests.

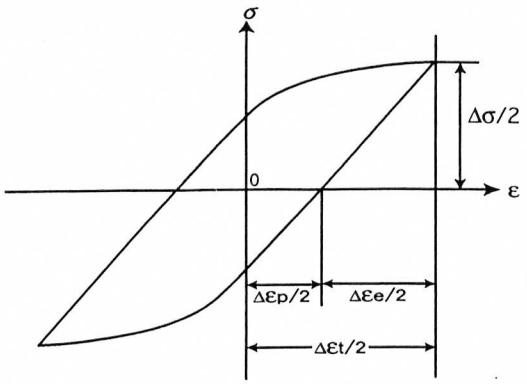

Fig. 3 A schematic representation of a hysteresis loop and the associated nomenclature.

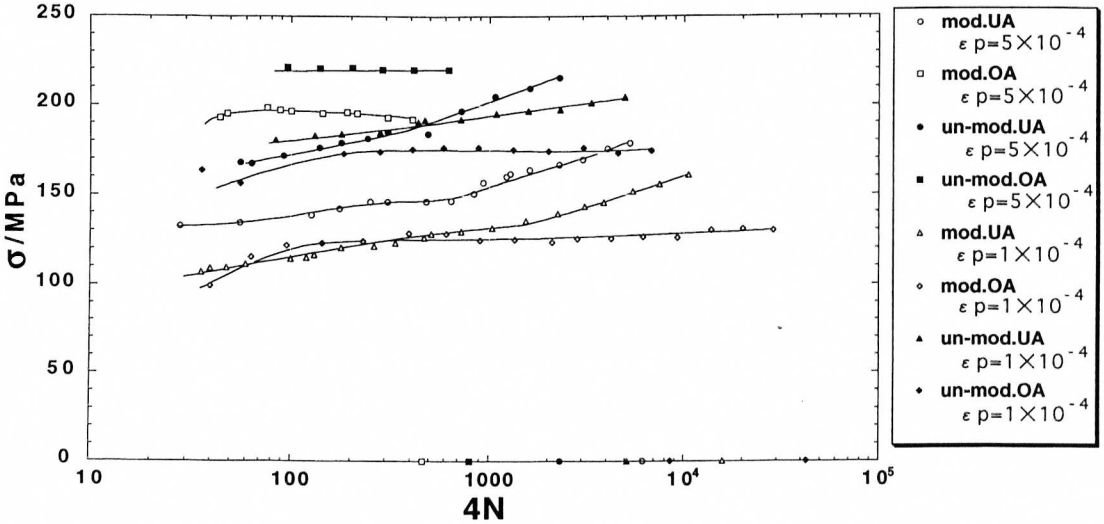

Fig. 4 Cyclic hardening behavior of the castings cyclically deformed at the constant plastic amplitude in the fully-reversed mode.

frequency of 1 Hz until final fracture. The stress-strain hysteresis loops were monitored continuously using an oscilloscope and were periodically recorded on the X-Y recorder. A schematic representation of a hystresis loop and the associated nomenclature is shown in Fig. 3. $\Delta\sigma/2$, $\Delta\varepsilon_e/2$, $\Delta\varepsilon_p/2$ and $\Delta\varepsilon_t/2$ denote the stress amplitude, the elastic, plastic and total strain amplitude, respectively. In this paper, $\Delta\sigma/2$ and $\Delta\varepsilon_p/2$ are labeled as σ and ε_p hereinafter. Morphological change of the specimen surface during cycling was monitored using a plastic replica and observed using an optical microscope. The specimen surface and the fracture surface were also observed using a scanning electron microscope.

3. RESULTS AND DISCUSSION

Low cycle fatigue tests were performed for two plastic strain amplitude levels ($1x10^{-4}$ and $5x10^{-4}$). Figure 4 shows the obtained relationship between the peak stress of the hystelesis loop (σ) and 4N, where N is the number of cycles. Arrows in the figure indicate the number of cycles for fracture (fatigue life). Cyclic hardening took place in all cases, but exhibiting different hardening behavior and stress levels depending on the eutectic Si particle morphology, aging condition and applied plastic strain amplitude. In the following sections, these cyclic hardening curves are compared by taking the cumulative strain $4N\varepsilon_p$ in stead of 4N to visualize the effects of plastic strain amplitude and the effects of microstructures as well.

Figure 5 shows the relationship between the σ and cumulative strain $4N\varepsilon_p$ for the un-modified OA and the modified OA. The unmodified specimens containing coarse irregular needle-like eutectic Si particles exhibited higher σ than the modified. This is in accordance with the higher flow stress of the unmodified specimens in the monotonic stress-strain curves (Fig. 2).

Cyclic hardening curves are compared between the modified OA and UA in Fig. 6. Gradual increase in σ with increase in the cumulative strain was observed for the UA. In contrast σ reached a stable saturation value in the OA after a relatively short initial cyclic hardening. The stress level is, then, higher for the OA than the UA in the cyclic range in Fig. 6.

Figures 7 (a) (b) show the effects of applied plastic strain amplitude for the UA and OA, respectively. No substantial increase of σ was observed by increase in ε_p in the UA. In the OA, however, the saturated stress amplitude levels increased with the increase in ε_p.

For wavy slip materials with a high stacking fault energy and a strong propensity for cross slip, such as aluminum alloys, only the plastic strain amplitude and test temperature influence the flow characteristics in fatigue. The fcc materials generally exhibit a cell structure at steady state, in which σ takes a constant value, σ_s, regardless of the dislocation structure which existed before cyclic straining. The cell size, which is independent of the history of material, decreases with increasing plastic strain amplitude. The empirical relationship, $\sigma_s \propto 1/\lambda$, is known for the dependence of saturation stress on cell size (λ) [3]. This is considered to hold for the OA materials which containing unshearble β', while for the UA the precipitates are easily sheared by dislocations, which may hinder homogeneous slip to form the cell structure. This is considered to result in no saturation characteristics in the UA as shown in Fig. 7 (a).

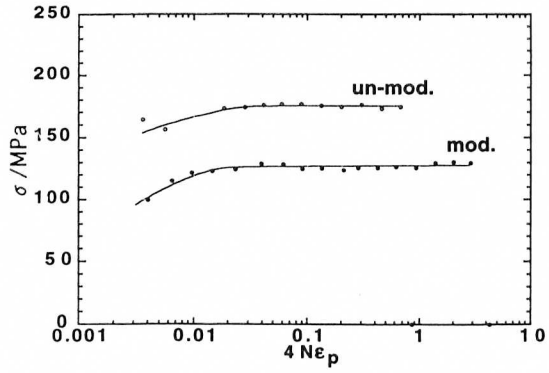

Fig. 5 Relationship between σ and cumulative strain $4N\varepsilon_p$ for the un-modified OA and the modified OA.

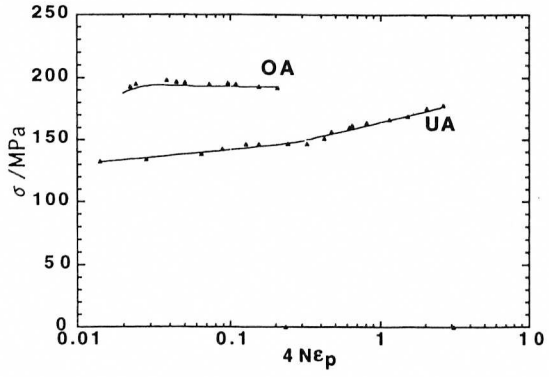

Fig. 6 Relationship between σ and cumulative strain $4N\varepsilon_p$ for the modified OA and UA.

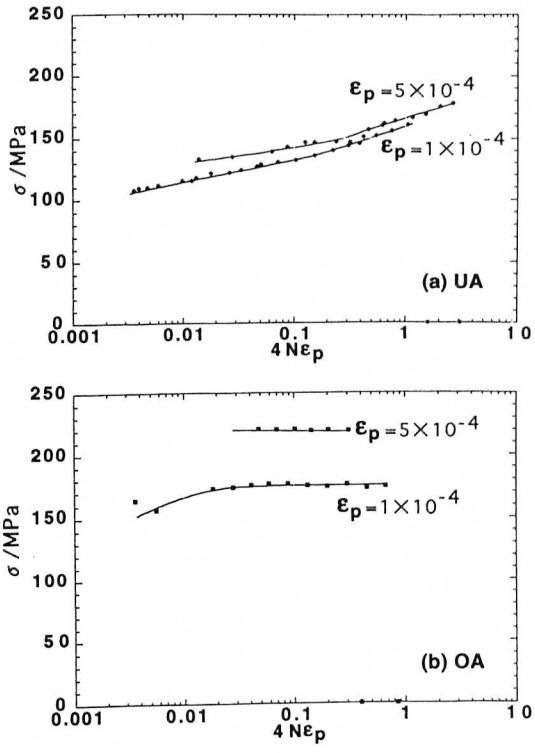

Fig. 7 Effects of applied plastic strain amplitude on cyclic hardening behavior.
(a) UA
(b) OA

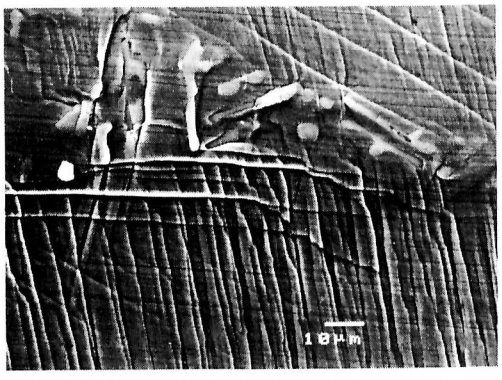

(a) UA

(b) OA

Fig. 8 Slip band morphology appeared on the specimen surface.

Slip band morphology appeared on the specimen surface of the cyclically deformed UA and OA were shown in Figs. 8 (a) (b) for comparison. Compared to the distinct arrays of the slip steps in the UA, the slip steps in the OA are wavy and vague. From this difference homogeneous cyclic deformation is anticipated in the UA.

4. CONCLUSIONS

Low cycle fatigue tests were performed for two plastic strain amplitudes in sand cast and HIPed Al-Si-Mg base cast aluminum alloys. Cyclic hardening took place in all the tests; however, different hardening behavior were obtained depending on the eutectic Si particle morphology, matrix aging condition and applied plastic strain amplitude. In contrast to the gradual increase in σ with increase of the cumulative strain in the UA, σ reached a stable saturation value and the σ increased with the applied strain amplitude in the OA. The saturation behavior together with the slip step morphology suggests formation of cell structure in the OA.

REFERENCES

[1] T. L Reinhart: ASM Handbook, 19 (1996) 813.

[2] Y. Ochi and R. Shibata: Proc. of the 93rd Conf. of Japan Institute of Light Metals, (1997) 137.

[3] Suresh: *Fatigue of materials*, Cambridge University Press, Cambridge, (1991) 10.